Lawrence Berkeley National Laboratory

Title

Engineering the atomic structure of sequence-defined peptoid polymers and their assemblies

Authors

Xuan, Sunting
Zuckermann, Ronald N

Engineering the Atomic Structure of Sequence-defined Peptoid Polymers and Their Assemblies

Sunting Xuan[a,b] and Ronald N. Zuckermann[a,b*]

aMolecular Foundry, Lawrence Berkeley National Laboratory, Berkeley, CA 94720

bMaterials Sciences Division, Lawrence Berkeley National Laboratory, Berkeley, CA 94720

Abstract

Peptoids are a family of sequence-defined, non-natural biomimetic polymers which show excellent properties including good chemical and enzymatic stability and high structural tunability. The solid-phase submonomer synthesis method allows precise control over the identity and sequence of chemically diverse side chains, enabling the atomic engineering of their chemical structures for a variety of applications. This unprecedented level of structural control enables access to atomically defined three-dimensional chain conformations and assemblies, facilitating the design and optimization of a variety of nanoscale architectures that can function in biology and materials science. In order to approach the rational design of peptoid materials in a more predictive and precise manner, it is crucial to fully understand how chemical information, in the form of the monomer sequence, encodes their folding and assembly into structurally defined, functional 3D shapes. This perspective focuses on recent studies into the atomic engineering of peptoid nanostructures by examining the impact of sequence variations on their secondary and three-dimensional structures, as well as their functional properties.

1. Introduction

Natural biopolymers such as proteins and nucleic acids have precisely defined monomer sequences which endow them with the informational, structural and functional complexity necessary to support life. Sequence changes of even a single amino acid in a protein can influence its three-dimensional structure, binding specificity or catalytic activity.[1, 2] Inspired by nature, considerable efforts have been devoted to the design and synthesis of synthetic polymers that are sequence-defined, aiming to ultimately engineer the structures, properties, and functions at the atomic level by tailoring the monomer sequences.[3-6] This would enable a new class of materials with the sophistication of biopolymers, but with improved stability and expanded chemistry. However, despite much effort, there are relatively few synthetic polymers for which this level of sequence control is synthetically feasible, while also achieving significant molecular weights. Among the most promising are poly(*N*-substituted glycines) (a.k.a. peptoids), which have attracted growing interest due to their synthetic accessibility, structural tunability, biocompatibility, and chemical and enzymatic stability.[7-9]

Peptoids are a class of synthetic biomimetic heteropolymers with the side chains appended to the nitrogen rather than the α-carbon as in peptides. Compared to peptides, peptoids lack hydrogen-bond donors and chiral centers along their backbones, which makes their structure and properties dominated by the side-chain chemistry and monomer sequence.[7, 8] This simple structural change also renders

peptoids with excellent thermal processability, good solubility in common solvents, and enhanced chemical and enzymatic stability.[8-11] Because of their polar amide backbone and a similar density of sidechains to peptides, peptoids are biocompatible and exhibit varied biological activities.[12] Studies have shown that peptoids exhibit minimal cytotoxicity[13, 14], good cellular permeability[15] and low immunogenicity[16]. Peptoids have shown promise as drug and gene delivery vehicles[17, 18], antifouling materials[19, 20], antimicrobial agents[21-23], anti-cancer therapeutics[14], antibody mimetic scaffolds for molecular recognition[24], and as a tissue-engineering scaffold[13] among others. Several review articles with particular emphasis on the biological applications of peptoids have been published in recent years.[25, 26]Although peptoids lack hydrogen-bond donors and chiral centers on their backbones, they nonetheless can fold or assemble into well-defined nanostructures that mimic some of the fundamental aspects of the structures and functionalities found in nature.[7, 27, 28] The focus of this perspective will be on recent studies on the atomic engineering of sequence-defined peptoid nanostructures, and in particular, the ability to tune their structure and function by creating subtle variations in the peptoid sequence. These efforts collectively aim to bring the folding paradigm of biology, and the precision of protein engineering, to synthetic materials. Peptoid research from a broad set of investigators is successfully demonstrating that the programming of chemical information into synthetic polymer chains is a practical synthetic route to rival the architectural and functional complexity found in proteins. We are at an exciting time in the advent of peptoid-based materials, where universal design rules that govern peptoid folding and assembly are emerging, that should inspire further development of nanostructured peptoid materials in a more predictable and precise manner.

2. Synthesis of sequence-defined peptoids

From a synthetic point of view, compared to most synthetic polymers, the chemical structures of peptoids are highly engineerable and controllable. The development of the step-wise but highly efficient solid-phase submonomer synthesis method in 1992, enabled ready access to a variety of sequence-defined peptoids with controlled chain length and near absolute monodispersity.[8, 29, 30] The method employs an iterative two-step monomer addition cycle, using cheap, simple building blocks, and no main chain protecting groups (Figure 1).[8] The first step is an acylation reaction of a resin-bound amine with bromo- or chloroacetic acid, and the second step is a nucleophilic substitution reaction with a primary amine submonomer.[8, 29, 30] The key synthetic synthons for peptoids, primary amines, are chemically diverse and readily available. Thus, a wide variety of side chains (e.g., ionic[31], aliphatic[10, 32], aromatic[33, 34], heterocyclic[21, 22, 35] and chiral[36, 37] etc.) can be incorporated to peptoids. In addition, the high-throughput "split-and-pool" combinatorial approach allows the synthesis of very large libraries of peptoid sequences simultaneously, such that a single bead contains a single unique sequence.[38-40] This synthesis method combined with a functional screen and a mass spectrometry-sequencing method,[41] allows the efficient identification of the "hit" sequence for specific applications. This method has been successfully applied to discover high-affinity peptoid ligands for numerous pharmaceutically relevant receptors[38, 40, 42, 43] .
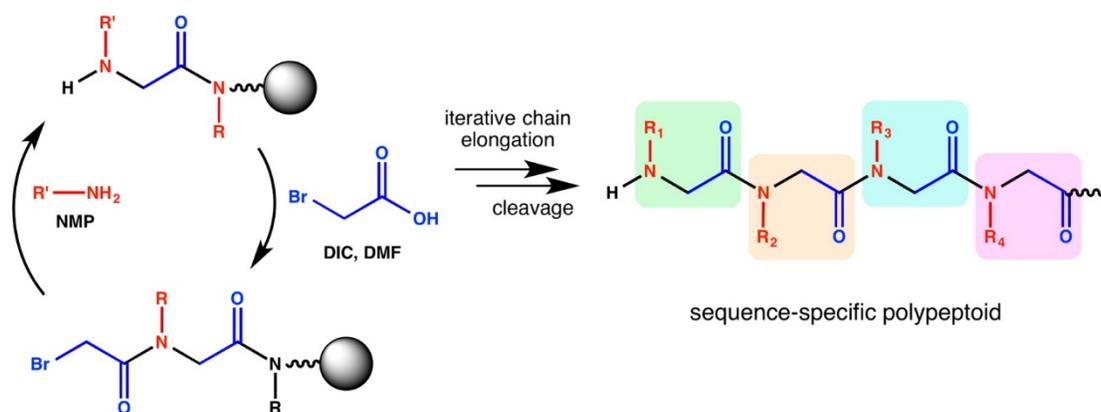
Figure **1**. The solid-phase submonomer synthesis method allows the rapid synthesis of a large diversity of sequence-defined peptoids using an iterative two-step monomer addition cycle of acylation followed by nucleophilic displacement with primary amines. Reproduced with permission from ref. [8]. Copyright (2013) American Chemical Society.

3. Peptoid structures: single chain conformations and assemblies

Peptoids have the capacity to form single-chain folded structures, assemble into supramolecular structures, and phase-separate/crystallize into different bulk morphologies, depending on their monomer sequence and solution conditions. Despite lacking hydrogen-bond donors and chiral centers along their backbones as found in natural polypeptides, investigators have revealed several key strategies to control their structure. It has been shown that individual peptoid chains in solution can fold into a variety of robust secondary structures such as helices[36, 44], ribbons[45], and square-helices[46] depending on their side chain chemistry and monomer sequence. Peptoids can also phase-separate, crystallize, and self-assemble into a variety of structures through intra- and inter-molecular interactions. Amphiphilic peptoids, especially diblock copolypeptoids, are well-known to phase-separate into lamellar morphologies in bulk.[10, 47-50] In solution, they have been shown to self-assemble into different structures including nanosheets[34, 51-54], nanotubes[55, 56], vesicles[57, 58], superhelices[59], and spherical micelles[60]. For example, peptoids bearing alternating hydrophobic and ionic hydrophilic side chains can form highly ordered, free-floating nanosheets through collapse of an intermediate monolayer formed at the air-water interface.[31] Diblock copolypeptoids containing a hydrophilic block and a hydrophobic block have also been shown to form free-floating crystalline nanosheets in solution driven by the crystallization of the hydrophobic block.[34, 51] In both types of nanosheets, the peptoid chains adopt extended conformations (*cis*-sigma strand) that pack face-to-face into rectangular lattices. This recently discovered packing rule is poised to guide the future design of peptoid nanostructures more predictively and precisely.

4. Backbone conformations of peptoids

In order to predictively design peptoid-based nanoarchitectures, it is essential to understand the conformation preferences of the backbone. Researchers have studied this in detail for decades, and their structural propensities are now quite well understood[61]. Peptoids are structurally distinct from peptides in three major ways: the peptoid backbones have no hydrogen bond donor or chiral center, and they are composed of tertiary amide bonds that have nearly isoenergetic *cis* ($\omega \approx 0^{\circ}$) and *trans* ($\omega \approx 180^{\circ}$) conformations. Thus, peptoids have intrinsic conformational preferences different than that of peptides.

The folded structure of a peptoid chain can be explicitly defined by understanding its backbone bond rotational preferences, which consist of three dihedral angles (ϕ, ψ, and ω). To better understand the distribution of these dihedrals, we recently analyzed 46 high quality, experimentally determined peptoid structures reported in literature. We found that the backbone dihedral angle pairs (ϕ and ψ) all fall within the expected, calculated energy minima of the peptoid Ramachandran plots derived from both *cis* and *trans* amide conformations (Figure 2)[61] Interestingly, only two regions of the plot were found to be populated. These regions are referred to as the Z_R and Z_S conformations, and because of the achirality of the peptoid backbone, these two regions are mirror images of each other (Figure 2). Since these minima are present for both the *cis* and *trans* amides, this means that there are only four predominant conformations that comprise peptoid structures (Z_{Rc}, Z_{Rt}, Z_{Sc}, and Z_{St}). These preferences provide guidance for the design of folded structures in a more predictive way. Manipulation of the backbone dihedral angles by engineering the chemistry and position of side chains is enabling the *de novo* design of folded peptoids with predictable and precise three-dimensional structures and functional properties.

Interestingly, while peptoid chains undergo *cis-trans* isomerization in solution due to their near isoenergetic states, in the solid state or in supramolecular assemblies, the amides have been shown to predominantly adopt the *cis* conformation, as evidenced by the X-ray scattering, cryo-TEM, NMR spectroscopy, and molecular dynamics simulations.[51, 62-64] This is due to the fact that *cis* conformation is more compact along the backbone direction than the *trans* conformation enabling a higher density of intra- and intermolecular interactions, as evidenced by the MD simulation.[62, 63] By alternating between the Z_{Rc} and Z_{Sc} conformations, the all-*cis* backbone can adopt an extended structure where the side chains are displayed on opposed faces. This fold is referred to as the *cis*-sigma strand and it has been observed in all the peptoid polymer crystals and in many supramolecular nanostructures reported, regardless of the chemistry of side chains.[62] These insights on the backbone conformation of peptoids lay the foundation for the rational design of functional biomimetic nanoarchitectures.
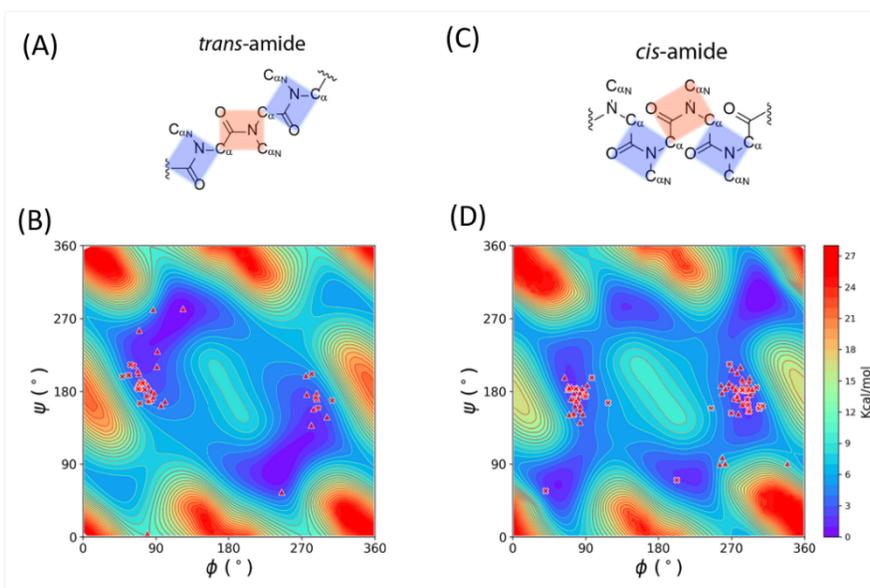
Figure **2**. Ramachandran plots of peptoids representing ϕ and ψ from 0^0 to 360^0. (A) Line drawing of *trans*-amide backbone conformations in peptoids. (B) Free-energy plot of trans disarcosine and ϕ and ψ combinations derived from *trans*-amide conformations in peptoid X-ray crystal structures (▲) and NMR structures (X). (C) Line drawing of *cis*-amide backbone conformations in peptoids. (D), Free-energy plot of cis disarcosine and ϕ and ψ combinations derived from *cis*-amide conformations in peptoid X-ray crystal structures (▲) and NMR structures (X). Adapted with permission from Ref. [61] Copyright (2019) John Wiley and Sons.

5. Atomic engineering of peptoids and their assemblies

The atomic-level synthetic control over the chemical structures of peptoids enables a fine degree of control over the backbone dihedral angles (ψ, ϕ, ω) to manipulate their chain conformations. The precise control over the chain length, sequence and side-chain identity of peptoids also greatly impact their crystallization, phase-separation, and self-assembly behaviors. Given these preferred backbone conformational preferences, researchers have been able to dramatically modulate peptoid properties by controlling the side chain sequence chemistry. Over the years, several structural classes have been identified and their sequence-dependencies studied. Here, we examine the ability of peptoids to form phase-separated morphologies in bulk, functional nanosheets, nanosheets, surface coatings and metalloprotein mimetics. Understanding the folding code and assembly rules associated with their essential structures and functions allow us to optimize their properties more precisely and predictively.

5.1. Engineering the phase-separated bulk morphologies of peptoids

Amphiphilic peptoids have the capacity to phase-separate in bulk. The precise control over the chemical structure of amphiphilic diblock copolypeptoids allows systematic investigation of the effect of monomer sequence on their phase-separation behavior. Segalman *et al*. reported the tunable phase behavior of diblock copolymers bearing a polystyrene block (PS) and a sequence-specific peptoid with 2-methoxyethyl side chains (Nme).[65] They showed that incorporation of a styrene-like residue, *N*-2-phenylethyl glycine (Npe), within the Nme block significantly decreased the segregation strength and therefore the order-disorder transitions of the diblock copolymers. We studied the phase separation of a series of diblock copolypeptoids, poly(*N*-2-(2-(2-methoxyethoxy)ethoxy)ethylglycine)-*b*-poly(*N*-(2-ethylhexyl)glycine) (Nte-*b*-Neh).[47] The total chain length was held at 36 while the volume fraction of pNte block (ϕ_{Nte}) was

systematically varied from 0.11 to 0.65. Interestingly, all the compounds, except the one with ϕ_{Nte} = 0.65, phase-separated to a lamellar morphology. We also studied the phase-separation behavior of diblock copolypeptoids bearing the same hydrophilic Nte block adjacent to a crystalline poly(*N*-decylglycine) (Ndc) block.[32, 62] All the samples studied phase-separated into a lamellar morphology with a rectangular crystal lattice. We found that the diblock copolypeptoids (Ndc-*b*-Nte) with an acetyl *N*-terminus exhibited a more ordered bulk morphology than its analogue with free amine *N*-terminus, presumably due to the difference in hybridization of the *N*-terminal amine atom (sp^3).[32]

5.2. Engineering the atomic structure of sheet- and tube-forming peptoids

Amphiphilic peptoids can self-assemble into either nanosheets[31, 34, 51] or nanotubes[55, 56] in solution depending on their chain length, side-chain chemistry and sequence. Nanosheets result from peptoids bearing alternating hydrophobic and hydrophilic ionic side chains or from amphiphilic diblock copolypeptoids. The propensity of these peptoids to form a planar, rectangular-like molecular shape with an extended backbone conformation (*cis*-sigma strand) and apposed side chain display, allows them to readily form rectangular lattices, hence the prevalence of nanosheets. Because these nanostructures are well-defined, we can essentially "mutagenize" their assembled structure, similar to the ability of the protein engineer tuning the structure of an enzyme. The solid-phase submonomer synthesis allows us to investigate the impact of atomic structural change on their self-assembled structures and functional properties.

5.2.1. Engineering the atomic structure of nanosheet interior

We initially discovered that peptoids with a sequence of alternating hydrophobic and hydrophilic ionic monomers can self-assemble into free-floating, highly ordered two-dimensional nanosheets.[31, 66, 67] The formation mechanism and atomic structure of the nanosheets have been well investigated.[68-70]. We also demonstrated that the nanosheets are readily engineerable in their hydrophobic interior through selective structural substitutions at the hydrophobic monomer positions. The nanosheet structure tolerated a wide variety of modifications to the *N*-2-phenylethyl side chain including many *meta* and *para* substituents.[33, 71] Photoreactive monomers were successfully introduced to the nanosheet sequence such that the sheets could be photo-crosslinked in their hydrophobic interior after their assembly to improve their chemical and mechanical stability.[72]

Recent advances in characterization tools such as X-ray scattering, cryo-TEM, and computational modeling greatly deepen the understanding of the assembled structures of peptoids at the atomic scale[51, 58, 62, 63, 69], and thus facilitate their atomic-engineering. X-ray scattering is a common technique widely used in polymer field. This technique, however, can only provide structural information in reciprocal space. Low-dose cryo-TEM, combined with single particle analysis methods, has emerged as an ideal technique to directly image soft materials in position space, though many challenges remain.[51] Single particle analysis is widely used in structural biology to solve protein structures.[73] It is an image processing technique used to improve the resolution of TEM images by analyzing and aligning numerous low signal-to-noise ratio images obtained under low-dose conditions.[73] In addition, different force fields, such as PEPDROID[74], MFTOID[63] and CGenFF[75], have been developed to facilitate accurate molecular dynamics (MD) simulations of peptoid structures. Using the feedback between precise synthesis, cryo-

TEM imaging, and MD simulations, we can now begin to engineer peptoid structures with the same atomic precision that structural biologists use to tune protein structure and function.

We have shown that we can directly observe the heterogeneity of chain packing within peptoid nanosheets assembled from poly(*N*-decylglycine)-*b*-poly(*N*-2(2-(2-methoxyethoxy)ethoxy)ethylglycine) (Ac-pNdc-*b*-pNte), in position space using cryo-TEM. Recently, in a related system with aromatic side chains, we were able to clearly image individual molecules within the nanosheet lattice. These aromatic nanosheets are highly crystalline with a ~60°C higher melting temperature than that of the Ac-pNdc-*b*-pNte nanosheets, which facilitated the characterization of their atomic structures using cryo-TEM and X-ray scattering. We demonstrated that substituents could be introduced onto the aromatic groups and varied without disrupting the packing preferences within the lattice.[76] We synthesized a series of diblock copolypeptoid decamers composed with the same hydrophilic poly(*N*-2(2-(2-methoxyethoxy)ethoxy)ethylglycine) (pNte) block and different *N*-2-phenylethylglycine-based hydrophobic blocks bearing a systematic series of aromatic ring substituents, varying in size and their electron withdrawing or donating character (Figure 3A). These sequence variants all formed free-floating 2D monolayer nanosheets. The crystal structures of nanosheets were well-characterized by a combination of cryo-TEM, X-ray scattering and MD simulations. Not only individual peptoid chains but also their relative packing orientations were directly observed by cryo-TEM at 1.5 Å resolution (Figure 3D). Bromine atoms at the *para* position of the aromatic side chains were directly visualized by cryo-TEM (Figure 3D), revealing atomic details in position space inaccessible by conventional scattering techniques. Interestingly, the organization of the chains within their crystal lattices were very similar, allowing subtle changes in the structure to be directly compared to one another. The spacing of adjacent rows along the *c* direction (Figure 3C) increased from 16.2 to 18.2 Å as the size of *para* substituents of aromatic side chains increased from hydrogen to bromine. All the nanosheets shared the same rectangular crystal lattice, and MD simulation revealed that the peptoid backbone conformation (*cis*-sigma strand) for all the molecules was conserved with the backbone dihedral angles all falling within the conformational minima of the peptoid Ramachandran plots. However, some variations in chain packing were observed depending on the chemical structure. The projection of an individual peptoid chain (V shape) as seen from the top view of the nanosheet (Figure 3D and E), arranged into different packing geometries along the *c* direction (parallel vs. anti-parallel V) depending on the *para*-substituents. The exact driving force behind this phenomenon has not been fully elucidated yet. This systematic atomic-level engineering of a crystal lattice, directly observed by cryo-TEM, has only been previously done in biological materials such as proteins.
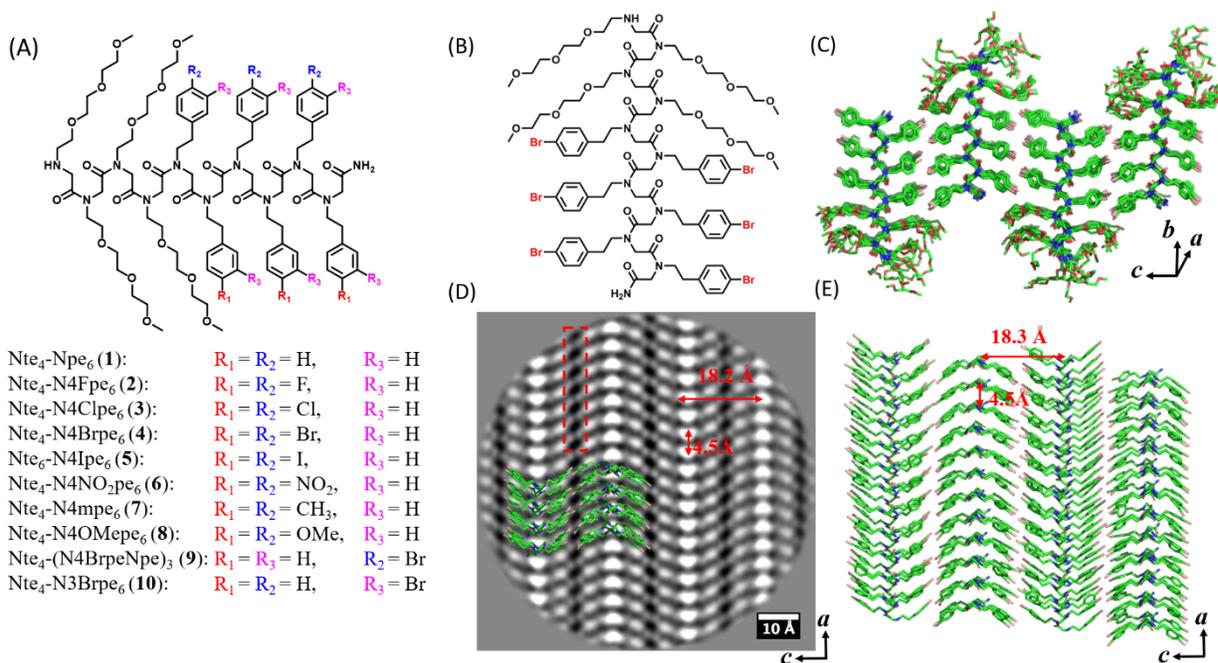
Figure **3**. Atomic engineering of nanosheets. (A) Chemical structures of diblock copolypeptoids with various *para*-substituents of aromatic side chains. (B) Chemical structures of Nte₄-N4Brpe₆ (**4**). (C) Molecular model of sheet **4**. The molecules are packed antiparallel along c direction and parallel along a direction. (D) Cryo-TEM image of sheet **4** from *b* direction (top view) showing anti-parallel V shapes along the *c* direction. The Br atoms showed a tip-to-tip packing (red box). (E) Top view of the hydrophobic domain in (C) from *b* direction showing anti-parallel V shapes along the *c* direction. The structure is overlapped with cryo-TEM image shown in (D).

5.2.2. Engineering the functionality of nanosheet exterior

Just as the crystal structure of the nanosheet interior can be engineered at the atomic level, the functionality of its solvent-exposed exterior (surface) of the nanosheet can also be tuned through engineering the polar side chains. Chen *et al*. incorporated a variety of functional moieties (e.g., crown ether for metal binding) at the *N*-terminus or side chain positions of the hydrophilic block of the sheet-forming diblock copolypeptoids, poly(*N*-2-carboxyethyl glycine)-*b*-poly(*N*-2-(4-chlorophenylethyl) glycine) (pNce-*b*-pN4Clpe), to display and pattern different functionalities on the surface of nanosheets.[34] Introducing conformationally constrained "loops" is also an ideal way to expose chemically diverse shapes on the nanosheet surface for different purposes. We previously covalently linked a pre-cyclized peptide to the *N*-terminus of the sheet-forming peptoid to display streptavidin-binding sites on the surface of the nanosheets.[66] We also inserted a variety of short, functional sequences to the middle of the sheet-forming peptoids to form nanosheets with a high density of loops exposed on the surface.[24, 77] Depending on the sequences inserted, these loops can mimic the multi-valent binding properties of antibodies to specifically proteins, serving as a potentially general platform for molecular recognition. Nanosheets with kinase-binding and gold-binding peptide loops exposed on the surface exhibited high affinity to protein casein kinase II (CK2α) and serves as templates for the growth of gold nanoparticles, respectively.[24] We also successfully introduced carbohydrate moieties on the nanosheet surface using different linker lengths on one of the hydrophilic side-chains, or within loops containing 2 to 6 hydrophilic peptoid monomers.[77] Both the linkers and loops contained one alkyne-bearing monomer, to which diverse carbohydrate units (e.g., mannose, *N*-acetylglucosamine and galactose) were covalently attached by copper-catalyzed azide-alkyne cycloaddition (CuAAC) reactions. Depending on the type of saccharides

displaced, nanosheets were able to selectively bind multivalent lectins, Concanavalin A and Wheat Germ Agglutinin. We also developed an even simpler nanosheet display method, where small-molecule lipid-conjugates could be co-assembled with sheet-forming peptoids to create a diversity of functionalized nanosheet bilayers with varying display functionality and densities.[78] These large-area multivalent 2D nanosheets on the micron scale could be ideal to combat pathogens by direct immobilization of entire organism in solution. We have demonstrated the ability of mannose-coated sheets to directly bind *E. coli* bacterial cells and inhibit their growth.[78]

Importantly, we found that the nanosheet surface loop display strategy described above was quite tolerant to sequence variation ~~within~~ in the loop. This is likely explained by the fact that the loops are solvated and surface exposed, thus they do not appreciably interfere with the molecular packing in the hydrophobic core. We therefore reasoned that the nanosheets could be used as a planar substrate upon which we could display diverse combinatorial libraries of loop variants, much like an antibody serves as a structural scaffold to display sequence diverse loops in its binding sites. Recently, we reported a method to prepare a library of nanosheets bearing a diversity of 6-mer peptoid loops, that could be screened against a variety of protein targets. [79] High affinity nanosheets were found to specifically bind to anthrax protective antigen ($(PA63)_7$). The sequence and chemistry of the hexapeptoid loops were designed to balance the overall water solubility and surface activity, promoting self-assembly and the correct folding of loops on the nanosheet surface. A basis set of 7 hydrophilic (**P**) and 13 hydrophobic (**H**) peptoid monomers, showing distinct chemical properties similar to the natural amino acids, were employed (Figure 4). We eliminated sequences that would likely interfere with the self-assembly mechanism, such as those with alternating **H** and **P** monomers, ≥ 3 **H** monomers, or with ≥ 2 large **H** monomers per sequence. In this way, a set of 256 specific sequences were synthesized to maximize the chemical distinctness of each loop. We prepared the nanosheet library simultaneously and in parallel at the milliliter scale using a pipetting method performed in multi-well plates with automated pipetting robot for high-throughput library generation and screening. "Hit" sequences which selectively bound to anthrax protective antigen $(PA63)_7$ were identified by a homogeneous fluorescence binding assay. The $(PA63)_7$-binding hit has a loop sequence, Namd-Ntyr-Ntyr-Ntyr-Ntyr-Namd, showing a "**PHHHHP**" pattern with four aromatic 2-(4-hydroxyphenyl)ethyl (Ntyr) side chains flanked by two polar carboxamidomethyl (Namd) side chains. Computer simulation of the loop-functionalized nanosheet indicated that the spatially dense display of loops enables high binding affinity to the target protein *via* multivalent interactions. The atomic control over the chemistry and sequence of loop peptoids combined with the high-throughput combinatorial screening method allow rapid and effective discovery of recognition elements for various pathogens (e.g., toxin proteins, viruses, and cells).
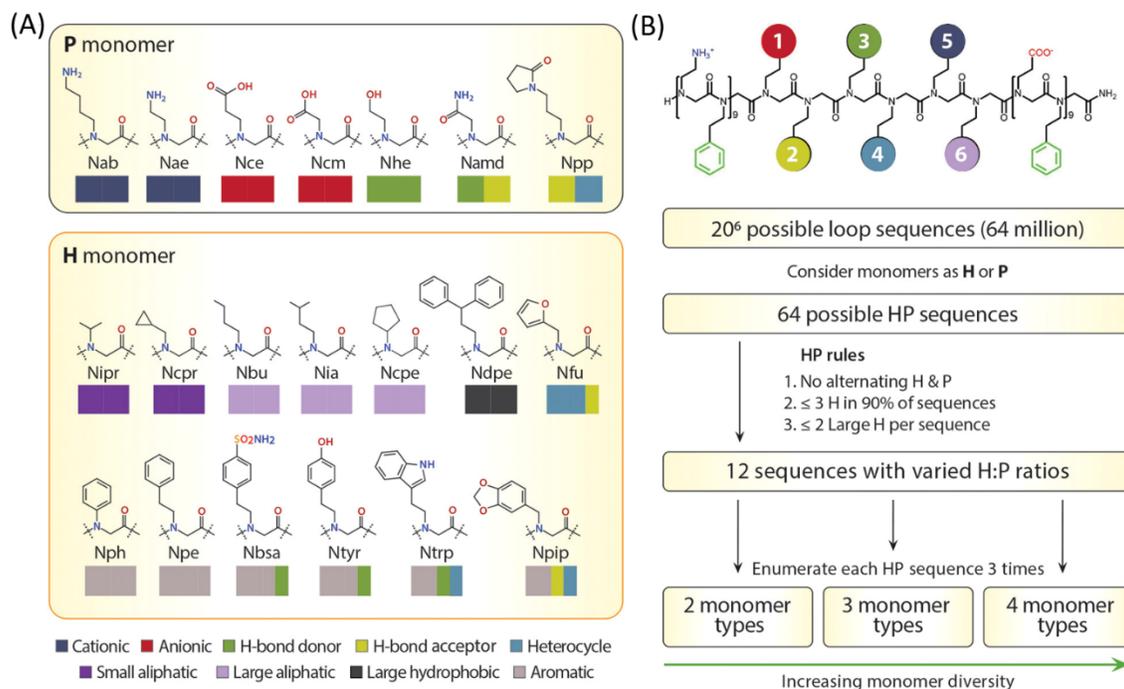
Figure 4. Design of the chemically diverse binding loops, built from a basis of 20 efficiently incorporated monomers. (A) **P** (hydrophilic) and **H** (hydrophobic) amine monomers exhibiting various properties. Colored rectangles represent primary and secondary properties of monomers. (B) Design algorithm for creating a maximally diverse set of loop insert sequences, while avoiding extremes of hydrophobicity. Reprinted with permission from Ref. [79]. Copyright (2020) American Chemistry Society.

5.2.3. Engineering the atomic structure of nanotube

The Ac-pNdc$_9$-*b*-pNte$_9$, as mentioned above, can form crystalline nanosheets in water. Interestingly, we found that increasing the length of the sequence to Ac-pNdc$_{13}$-*b*-pNte$_{13}$ and Ac-pNdc$_{18}$-*b*-pNte$_{18}$ led to the formation of crystalline nanotubes of uniform diameter.[55] Black stripes with 2.4 nm adjacent spacing along the nanotube axis, corresponding to the adjacent rows of backbones, were clearly visible by cryo-TEM. (Figure 5A-C). The spacing (2.4 nm) is nearly identical to that observed in the Ac-pNdc$_9$-*b*-pNte$_9$ nanosheet (Figure 5D-E)[51, 52], suggesting their similar packing between adjacent rows of backbones. The diameter of tubes increased from ~4.3 to ~9.3 nm as the chain length of peptoid increased from Ac-pNdc$_{13}$-*b*-pNte$_{13}$ to Ac-pNdc$_{18}$-*b*-pNte$_{18}$. Chen *et al*. discovered that in contrast to the 2-phenylethyl based diblock nanosheet, pNce-*b*-pN4Clpe,[34, 80] a benzyl analog of the same sequence, pNce-*b*-pNbpm, initially formed nanosheets followed by curving into single-walled stiff nanotubes.[56] Similarly, early studies by our group showed that longer amphiphilic diblock copolypeptoid, pNpe$_{15}$-*b*-pNce$_{15}$, initially formed nanosheets in water, which slowly transformed into homochiral left-handed superhelices.[59] The left-handed homochirality was remarkably robust that ~~either~~ introduction of chiral side chains or addition of chiral counterions could not change the overall superhelix chirality. It's remarkable that chain length and side chain length of peptoids have such a great impact on their self-assembled structures. ~~However, a~~ The fully understanding of the atomic structure of the nanotubes and superhelices as well as the driving force of their formation is lacking and needs further investigation.

10

Ac-pNdc₁₈-*b*-pNte₁₈

Ac-pNdc₉-*b*-pNte₉
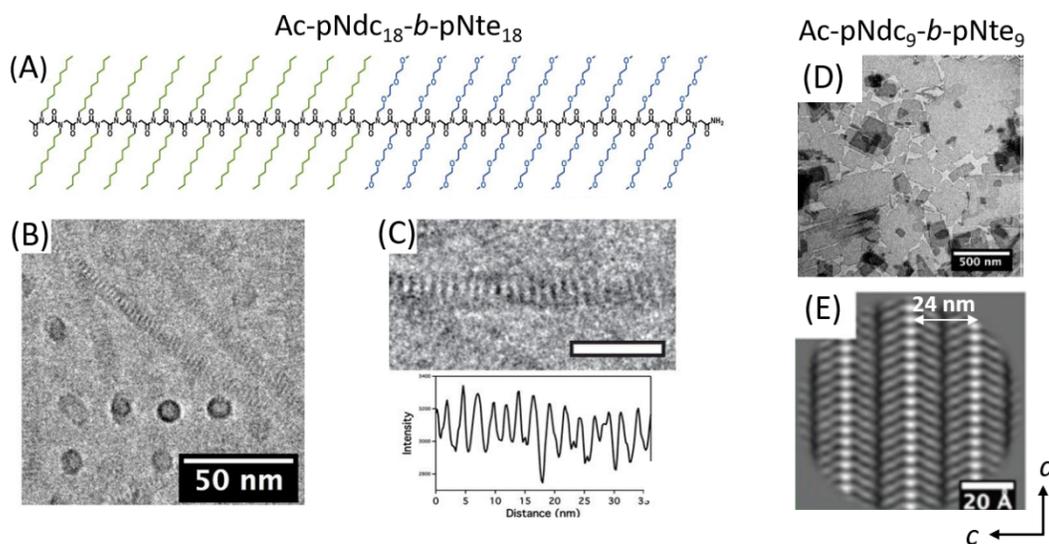
Figure 5. (A) Chemical structure of Ac-pNdc₁₈-*b*-pNte₁₈. (B) Cryo-EM 2D projection image shows nanotubes of uniform diameter in a vitrified thin film. (C) Cryo-EM close-up of a single nanotube (scale bar, 20 nm) shows regular latitudinal stripes (Top). A line profile along the longitudinal direction of the nanotube indicates a periodicity of 2.4 ± 0.2 nm (Bottom). (D) TEM images of nanosheets formed by Ac-pNdc₉-*b*-pNte₉. (E) Cryo-TEM image of the nanosheets showing a 24 nm spacing between adjacent rows of backbones along the *c* direction. (D) is adapted with permission from Ref. [51]. Copyright (2018) American Chemistry Society. (E) is adapted from Ref. [52]. with permission from The Royal Society of Chemistry.

5.3. Surface passivation with sequence-defined peptoids

The atomic structure of peptoids also greatly affect their interaction to various nanoscale substrates such as carbon nanotubes, DNA origamis and lipid vesicles.[81-83] We showed the deposition of functionalized loopoid monolayers with high degree of uniformity on planar hydrophobic substrates, including to the tip of glass optical sensing fibers, by a Langmuir-Schaefer method.[84] We demonstrated the successful display of globotriose- and peptide (TYWWLD)-functionalized loops on the surface of optical fibers which can detect the specific binding of the pathogen derived protein, shiga toxin and anthrax protective antigen. The Landry group reported the design, synthesis and evaluation of a series of amphiphilic peptoids of variable sequences, charges, polarities, and lengths to identify sequences that could be adsorbed to single-walled carbon nanotubes (SWNTs) with high stability (Figure 6).[81] They found that the stability of peptoid-coated SWNTs under a variety of conditions (e.g., ionic strength, protease exposure, and cell culture media) was dependent upon on the composition and length of peptoids. Chain hydrophilicity, high charge, and π-π interaction from aromatic side chains were found to be important contributors to the peptoid-SWNT adsorption efficiency. Repeats of (Nce-Npe) were identified as a highly stable peptoid sequence for SWNT stabilization at physiological pH. Peptoid-SWNT adsorption efficiency was roughly proportional to peptoid length, owing to the increased number of contacts between a longer peptoid and the SWNT surface. Incorporation of a lectin-binding 6-monomer loop sequence, consisting of three *N*-butylglycine (Nbu) and three *N*-(*N*-pyrrolidinonylpropyl)glycine (Npp) monomers (Nbu-Nbu-Bpp-Npp-Nbu-Npp), to the middle of an (Nce-Npe)₁₈ anchor sequence, was also shown to adsorb to the carbon nanotubes. The loops within this peptoid were shown to be surface exposed and interact semi-selectively with Wheat Germ Agglutinin (WGA), a sugar-binding lectin (Figure 6A).
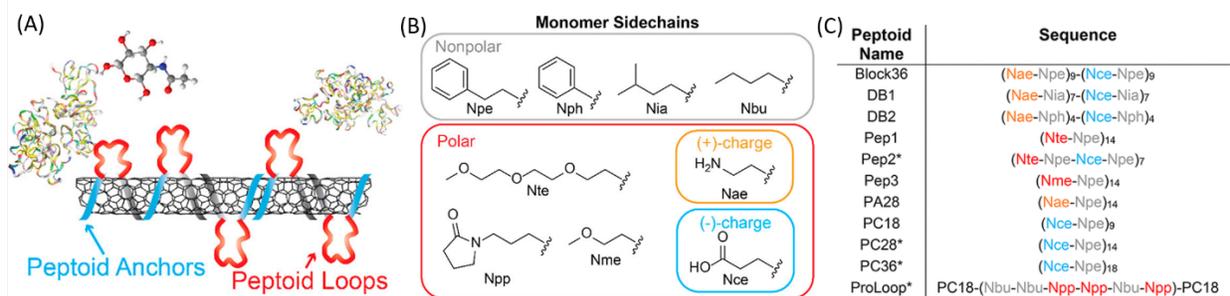
Figure **6**. Electrostatic assemblies of single-walled carbon nanotubes (SWNT) and peptoids. (A) A cartoon showing adsorption of peptoids onto the surface of SWNT with peptoid loops well displaced for the detection of a lectin protein. (B) Monomers used to create the peptoids in this study. (C) Library of 11 Peptoid structures tested for adsorption to SWNT. Peptoids denoted with an asterisk (*) successfully adsorb on SWNT to form peptoid-SWNT assemblies, while other peptoids do not suspend SWNT at pH 7. Adapted with permission from Ref. [81]. Copyright (2019) American Chemistry Society.

The Gang group demonstrated the stabilization of DNA origami nanostructures via the electrostatic adsorption of sequence-defined peptoids.[82] Adsorption of polycations onto the negatively charged DNA backbone *via* electrostatic interaction is a common approach to protect origamis against nuclease degradation and enhance transfection efficiency. However, there is limited understanding on how the charge density and charge distribution of polycations impact their interaction with DNA origamis. Sequence-defined peptoids, with atomically controlled structures, were identified as a great platform to investigate this impact. Thus, a series of peptoid sequence patterns composed of positively charged (Nae) and neutrally charged (Nte) moieties, varying charge density and distribution, were synthesized and systematically explored regarding their protection of DNA origami (Figure 7). It was found that the brush-type peptoid Nae_{12}-Nte_{12} (**PE2**) (Figure 7A) exhibited the best protection of DNA origamis in conditions including Mg^{2+} depletion and presence of degrading nuclease. This is attributed to the persistent multivalent interactions of Nce moieties with DNA spread across the DNA backbone (Figure 7C), as evidenced by the molecular dynamics (MD) simulations.
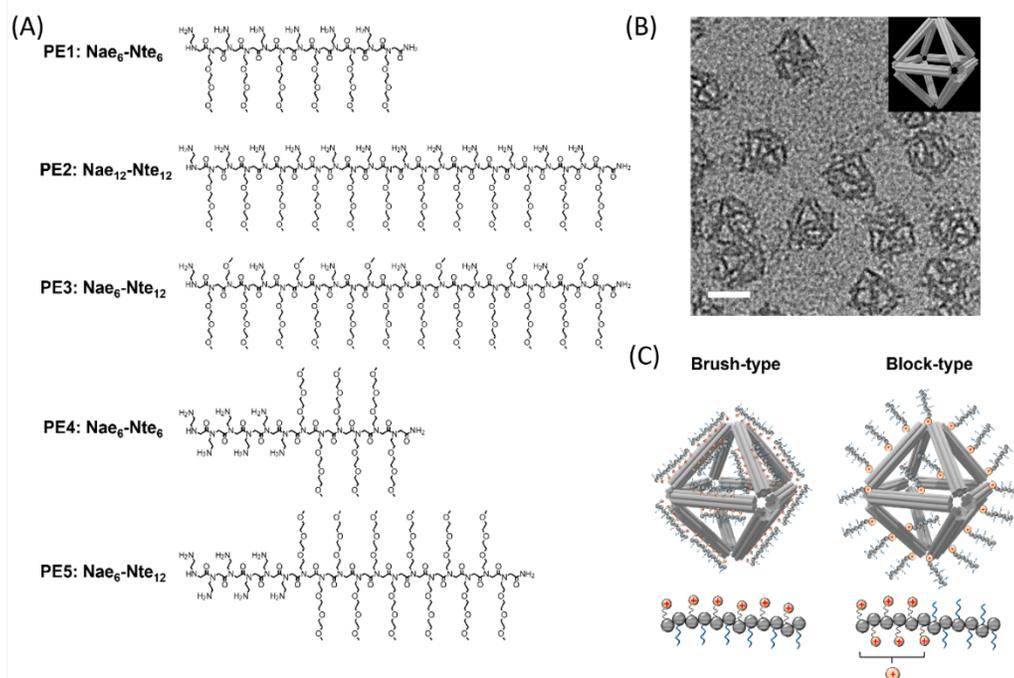
Figure **7**. Peptoids with different molecular architectures for DNA origami protection. (A) Chemical structures of peptoids designed to protect 3D octahedra-shaped DNA origamis (OC). **PE1**, **PE2** and **PE3** represent brush-type peptoids; **PE4** and **PE5** are block-type peptoids. Nae: *N*-(2-aminoethyl)glycine, Nte: *N*-2-(2-(2-methoxyethoxy)ethoxy)ethylglycine and Nme: *N*-(2-methoxyethyl)glycine. (B) TEM image and schematic view (inset) of the OC structure (scale bar: 50 nm). (C) Schematic view showing the different surface coating of the two types ("brush" and "block") of peptoids on the OC structure proposed in this work, which leads to varied protection effect.

5.4. Engineering the atomic structure of peptoid chain conformation

The preferred local conformational minima of peptoids in the Ramachandran plot as shown in Figure 2, combined with their excellent chemical and enzymatic stability, makes peptoids an ideal platform to design peptoids that can fold into single-chain, protein-like structures. One such approach takes advantage of peptoids that can serve as ligands for targeted metal coordination.[85-89] However, there are limited reports on metallopeptoids with atomically-defined structure in solution. The first examples of atomic structures of metallopeptoids were characterized in the solid-state using crystallography and not in solution.[90]. It is important to fully understand the atomic structures of metallopeptoids in solutions correlated to their *in situ* catalytic activities. Thus, through structural design, combinatorial high-throughput synthesis and subsequent screening of a library of peptoids, we discovered and optimized a series of peptoids oligomers (≤ 7 residues) that fold into a single stable conformation to provide unprecedented tetra-and hexadentate chelation to a tetrametallic $[Co_4O_4]$ cubane cluster *via* multiple simple carboxylate moieties.[91] The solution-phase structures of the peptoid-metalloclusters at the atomic-level were well-characterized by a combination of 2D NMR spectroscopy and molecular dynamics (MD) simulations. Inspired by the crystal structure of the multimetallic enzyme photosystem II (Figure 8a) showing that three carboxylate residue of a peptide sequence bind to the cubane cluster, we first synthesized a peptoid analogue of the C-terminal trimer peptide fragment, Asp-Leu-Ala-OH, as Fm-Ncm-Nbn-NAla-NH$_2$ (**H$_2$A**) (Fm = formyl, Ncm = *N*-carboxymethyl glycine, Nbn = *N*-benzyl glycine) (Figure 8b) to target two-face binding of the cobalt cubane. To remove the amide isomerization at each terminus, formyl was replaced with *p*-toluenesulfonyl (Ts) and NAla was changed to Ala-OH to obtain the Ts-Ncm-Nbn-Ala-OH (**H$_2$B**) (Figure 8b). Reaction of one and two equivalents of **H$_2$B** with the tetrametallic cobalt cluster,

Co₄O₄(OAc)Py₄, produced a single conformer with *cis*-amides of mono- and *bis*-peptoid complex (**1-B** and **1-2B**), respectively, as shown in Figure 8c the lowest energy NMR structures of **1-2B** determined by replica-exchange molecular dynamics (REMD). We also attempted to link the sequence of H₂B and a carboxylate residue Nce with a tripeptoid loop to allow carboxylate binding to the third face of cobalt cubane. We employed a combinatorial approach, the "split-and-pool" strategy, to synthesize a library of 125 resin-bond sequences varied at the loop positions and identified a predominant hit sequence, Ts-Nce-Nae-Nhe-Nrpe-Ncm-Nbn-Ala-OH (**H₃C**), by direct colorimetric analysis. The mono-peptoid complex of **H₃C** (**1-C**) exhibits ~ 51% of a single conformation. Single-site sarcosine mutations of each of the three loop residues revealed that the H-bond from Nae, and steric constraints of N*rpe*, are critical in decreasing backbone flexibility to rigidify the peptoid ligands for better binding. Looking forward, the target of the fourth face of the cubane, or even the pyridine faces, can be approached using this method combining both structural design and combinatorial screening. This efficient ligand design strategy holds promise for creating new scaffolds for the synthesis and manipulation of multimetallic cluster-base metalloenzyme mimics.
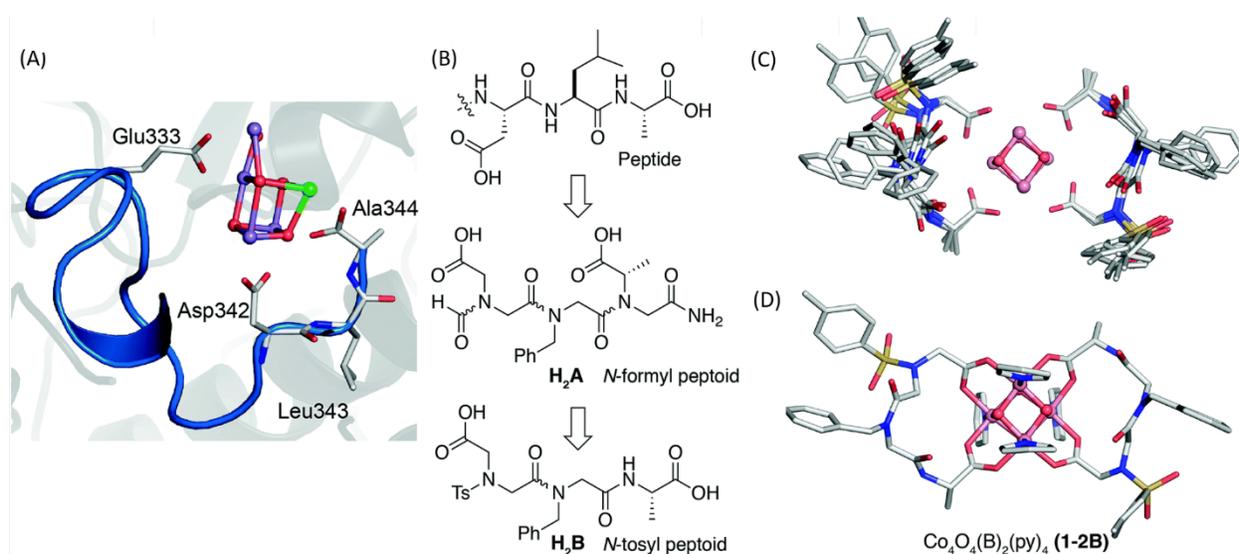
Figure 8. (A) Selected amino acid residues from the D1 subunit (blue) that bind to the Mn₄Ca oxygen-evolving complex (OEC). (B) Design of the peptoid analogues based on D1. (C) Ensemble of the five lowest energy NMR structures of **1-2B** (pyridine ligands omitted for clarity). (D) The lowest energy structure of **1-2B**. Reprinted from Ref. [91]. with permission from The Royal Society of Chemistry.

Controlling the *cis*- and *trans*-amide conformations (rotation about ω) in peptoid backbones is critical to rigidify the local conformation and thus control the folded structures of peptoids. Peptoid backbones preferentially generally adopt all *cis*-amide conformation in peptoid crystals regardless of the chemistry of side chains, as previously reported.[52, 62, 76] However, free in solution, peptoids undergo *cis-trans* isomerization due to the similar energy of the two conformers. A common strategy to induce one conformer over the other is to utilize local non-covalent interactions, including n→π*, steric, electronic, and hydrogen bonding interactions, to regulate the amide bond rotation of peptoid backbones.[92-94] Several side chains have been reported that are capable of enforcing a specific amide conformation. *N*-aryl side chains have been shown to strongly enforce *trans*-amide geometries in peptoid backbone.[45, 95, 96] Peptoids with extremely bulky and α-branched side-chains, such as chiral 1-naphthylethyl[95] and tert-butyl[93] side chains, adopt predominantly *cis*-amide conformation as the steric interaction present in the *trans*-amide conformation is disfavored. Triazolium and *N*-alkylpyridinium side chains also promote

cis-isomers *via* electronic interactions between backbone carbonyl and side-chain.[92, 94] These conformation-inducing side chains, however, often suffer from being either too hydrophobic, have low monomer addition yields, or are incompatible with acid cleavage in solid-phase synthesis. Surprisingly, hydrogen bonding in peptoids between the side-chain and the backbone carbonyl oxygen has not been widely recognized to promote the *cis*-amide isomers. Thus, we developed a novel class of water soluble peptoids, bearing cationic alkyl ammonium ethyl side chains, which showed the strongest enforcement of the *cis*-amide backbone conformation to date ($K_{cis/trans}$ up to 70) (Figure 9).[97] We demonstrated that the preference of *cis*-amide conformation is due to an unexpected ensemble of weak intramolecular CH-O and/or NH-O hydrogen bonds between the side-chain and the backbone carbonyl moieties, as evidenced by X-ray crystallography, variable-temperature NMR spectroscopy, and DFT calculations. Many of these alkylamino sidechains are commercially available or are obtainable *via* simple synthesis and can be readily functionalized. Furthermore, a propargyl group can be easily incorporated to the side-chain which allows further diversification of the side-chain through CuAAC "click" chemistry on resin. We further synthesized a water soluble 10mer with alternating hydrophobic *N*-aryl side chains (strong *trans*-inducers) and the newly developed hydrophilic cationic alkyl ammonium ethyl side chains (strong *cis*-inducers), mimicking the sequence which formed ribbon structure[45] reported by Blackwell *et al*. The ribbon structure with a pattern of alternating *cis*- and *trans*-amides was identified in polar protic solvents (MeOD and D$_2$O), as evidenced by ^{1}H NMR spectroscopy. This is, so far, the longest known peptoid sequence that can fold into ribbon structure.
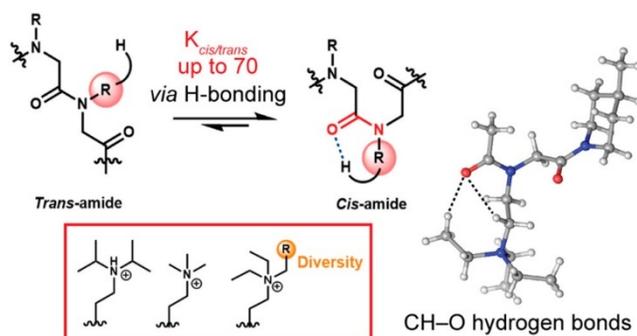
Figure **9**. Cationic alkyl ammonium ethyl side chains, highly diverse, induced *cis*-amide conformation of peptoids through an ensemble of weak CH-O hydrogen bonding. The K$_{cis/trans}$ could reach up to 70. Reprinted with permission from Ref. [97]. Copyright (2019) American Chemistry Society.

6. Conclusions and outlook

Peptoids, lacking hydrogen-bond donors and chiral centers along backbones, have intrinsic conformational preferences different than those of peptides. The structure and property of peptoids are predominantly determined by their chain length, side chain chemistry and monomer sequence. A comprehensive understanding on how the peptoid chemical structure impacts the dihedral angles of the peptoid backbone is needed in order to achieve the precise folding of peptoids into protein-like structures in a predictive way. Amphiphilic peptoids are known to self-assemble into a variety of supramolecular structures (e.g., nanotubes, nanosheets, vesicles and superhelix) *via* intra- and intermolecular interactions depending on their sequence. A clear understanding of their atomic structures, as well as their assembly mechanisms is a prerequisite to further precisely engineer their structure and function for specific

applications. Advances in the submonmer solid-phase synthesis enable chemists to readily access an enormous diversity of sequence-defined peptoids with precise control over their chain length, side-chain chemistry and sequence. The vast diversity and atomic-level precision of peptoid sequence offered by this synthetic method allow us to systematically investigate how the atomic modification of peptoid chemical structures impact their higher order structures as well as physicochemical and functional properties, paving the way to design peptoid materials that rival the structural and functional complexity found in nature. The intrinsic packing preferences of peptoid chains, as described above, can now be utilized to confer additional precision and hierarchical complexity to the nanostructures. For example, within a peptoid crystal lattice, voids could be created to form binding pockets, or functional groups could be introduced to certain side chains to introduce specific binding interactions or catalytic activities. Pairwise chemical or steric interactions between two polymers can be introduced to promote inter-chain complementarity like in DNA.[98] Overall, sequence-defined peptoids are an ideal platform for the generation of information-rich, folded and self-assembled nanostructures bearing molecular recognition sites, catalytic cites, stimuli-responsive properties and hierarchical architectures. Looking forward, the combination of automated synthesis, detailed structural characterization, molecular dynamics simulation and functional screening hold great promise to develop atomically-defined biomimetic nanostructures. The feedback obtained from the growing number of atomic structures will further deepen our understanding of the folding and assembly rules, and guide us to design peptoid materials more precisely and predictively.

Acknowledgements

References

[1] R. Bhattacharya, P.W. Rose, S.K. Burley, A. Prlić, Impact of genetic variation on three dimensional structure and function of proteins, PLoS One 12(3) (2017) e0171355.
[2] D. Lee, O. Redfern, C. Orengo, Predicting protein function from sequence and structure, Nat. Rev. Mol. Cell Biol. 8(12) (2007) 995-1005.
[3] P. Nanjan, M. Porel, Sequence-defined non-natural polymers: synthesis and applications, Polym. Chem. 10(40) (2019) 5406-5424.
[4] Y. Tao, Z. Wang, Y. Tao, Polypeptoids synthesis based on Ugi reaction: Advances and perspectives, Biopolymers 110(6) (2019) e23288.
[5] M.A.R. Meier, C. Barner-Kowollik, A New Class of Materials: Sequence-Defined Macromolecules and Their Emerging Applications, Adv. Mater. 31(26) (2019) 1806027.
[6] J. De Neve, J.J. Haven, L. Maes, T. Junkers, Sequence-definition from controlled polymerization: the next generation of materials, Polym. Chem. 9(38) (2018) 4692-4705.
[7] S. Xuan, R.N. Zuckermann, Diblock copolypeptoids: a review of phase separation, crystallization, self-assembly and biological applications, J. Mater. Chem. B (2020) https://doi.org/10.1039/D0TB00477D.
[8] J. Sun, R.N. Zuckermann, Peptoid Polymers: A Highly Designable Bioinspired Material, ACS Nano 7(6) (2013) 4715-4732.

[9] B.A. Chan, S. Xuan, A. Li, J.M. Simpson, G.L. Sternhagen, T. Yu, O.A. Darvish, N. Jiang, D. Zhang, Polypeptoid polymers: Synthesis, characterization, and properties, Biopolymers 109(1) (2018) e23070.

[10] A.M. Rosales, H.K. Murnen, R.N. Zuckermann, R.A. Segalman, Control of Crystallization and Melting Behavior in Sequence Specific Polypeptoids, Macromolecules 43(13) (2010) 5627-5636.

[11] S.M. Miller, R.J. Simon, S. Ng, R.N. Zuckermann, J.M. Kerr, W.H. Moos, Proteolytic studies of homologous peptide and N-substituted glycine peptoid oligomers, Bioorg. Med. Chem. Lett. 4(22) (1994) 2657-2662.

[12] N. Gangloff, J. Ulbricht, T. Lorson, H. Schlaad, R. Luxenhofer, Peptoids and Polypeptoids at the Frontier of Supra- and Macromolecular Engineering, Chem. Rev. 116(4) (2016) 1753-1802.

[13] S. Xuan, C.-U. Lee, C. Chen, A.B. Doyle, Y. Zhang, L. Guo, V.T. John, D. Hayes, D. Zhang, Thermoreversible and Injectable ABC Polypeptoid Hydrogels: Controlling the Hydrogel Properties through Molecular Design, Chem. Mater. 28(3) (2016) 727-737.

[14] Y. Luo, Y. Song, M. Wang, T. Jian, S. Ding, P. Mu, Z. Liao, Q. Shi, X. Cai, H. Jin, D. Du, W.-J. Dong, C.-L. Chen, Y. Lin, Bioinspired Peptoid Nanotubes for Targeted Tumor Cell Imaging and Chemo-Photodynamic Therapy, Small 15(43) (2019) 1902485.

[15] P.A. Wender, D.J. Mitchell, K. Pattabiraman, E.T. Pelkey, L. Steinman, J.B. Rothbard, The design, synthesis, and evaluation of molecules that enable or enhance cellular uptake: Peptoid molecular transporters, Proc. Natl. Acad. Sci. 97(24) (2000) 13003-13008.

[16] D. Meister, S.M. Taimoory, J.F. Trant, Unnatural amino acids improve affinity and modulate immunogenicity: Developing peptides to treat MHC type II autoimmune disorders, Pept. Sci. 111(1) (2019) e24058.

[17] A. Li, D. Zhang, Synthesis and Characterization of Cleavable Core-Cross-Linked Micelles Based on Amphiphilic Block Copolypeptoids as Smart Drug Carriers, Biomacromolecules 17(3) (2016) 852-861.

[18] Y. Song, M. Wang, S. Li, H. Jin, X. Cai, D. Du, H. Li, C.-L. Chen, Y. Lin, Efficient Cytosolic Delivery Using Crystalline Nanoflowers Assembled from Fluorinated Peptoids, Small 14(52) (2018) 1803544.

[19] S. Xuan, S. Gupta, X. Li, M. Bleuel, G.J. Schneider, D. Zhang, Synthesis and Characterization of Well-Defined PEGylated Polypeptoids as Protein-Resistant Polymers, Biomacromolecules 18(3) (2017) 951-964.

[20] K.H.A. Lau, C. Ren, T.S. Sileika, S.H. Park, I. Szleifer, P.B. Messersmith, Surface-Grafted Polysarcosine as a Peptoid Antifouling Polymer Brush, Langmuir 28(46) (2012) 16099-16107.

[21] N.P. Chongsiriwatana, J.A. Patch, A.M. Czyzewski, M.T. Dohm, A. Ivankin, D. Gidalevitz, R.N. Zuckermann, A.E. Barron, Peptoids that mimic the structure, function, and mechanism of helical antimicrobial peptides, Proc. Natl. Acad. Sci. 105(8) (2008) 2794-2799.

[22] B. Mojsoska, R.N. Zuckermann, H. Jenssen, Structure-Activity Relationship Study of Novel Peptoids That Mimic the Structure of Antimicrobial Peptides, Antimicrob. Agents Chemother. 59(7) (2015) 4112-4120.

[23] A. Andrea, N. Molchanova, H. Jenssen, Antibiofilm Peptides and Peptidomimetics with Focus on Surface Immobilization, Biomolecules 8(2) (2018) 27.

[24] G.K. Olivier, A. Cho, B. Sanii, M.D. Connolly, H. Tran, R.N. Zuckermann, Antibody-Mimetic Peptoid Nanosheets for Molecular Recognition, ACS Nano 7(10) (2013) 9276-9286.

[25] K.H.A. Lau, Peptoids for biomaterials science, Biomater. Sci. 2(5) (2014) 627-633.

[26] J. Sun, Z. Li, 7 - Peptoid applications in biomedicine and nanotechnology, in: S. Koutsopoulos (Ed.), Peptide Applications in Biomedicine, Biotechnology and Bioengineering, Woodhead Publishing2018, pp. 183-213.

[27] S.A. Fowler, H.E. Blackwell, Structure–function relationships in peptoids: Recent advances toward deciphering the structural requirements for biological function, Org. Biomol. Chem. 7(8) (2009) 1508-1524.

[28] A. Battigelli, Design and preparation of organic nanomaterials using self-assembled peptoids, Biopolymers 110(4) (2019) e23265.

[29] R.N. Zuckermann, J.M. Kerr, S.B.H. Kent, W.H. Moos, Efficient method for the preparation of peptoids [oligo(N-substituted glycines)] by submonomer solid-phase synthesis, J. Am. Chem. Soc. 114(26) (1992) 10646-10647.

[30] R.N. Zuckermann, Peptoid origins, Pept. Sci. 96(5) (2011) 545-555.

[31] E.J. Robertson, A. Battigelli, C. Proulx, R.V. Mannige, T.K. Haxton, L. Yun, S. Whitelam, R.N. Zuckermann, Design, Synthesis, Assembly, and Engineering of Peptoid Nanosheets, Acc. Chem. Res. 49(3) (2016) 379-389.

[32] D.R. Greer, M.A. Stolberg, S. Xuan, X. Jiang, N.P. Balsara, R.N. Zuckermann, Liquid-Crystalline Phase Behavior in Polypeptoid Diblock Copolymers, Macromolecules 51(23) (2018) 9519-9525.

[33] E.J. Robertson, C. Proulx, J.K. Su, R.L. Garcia, S. Yoo, E.M. Nehls, M.D. Connolly, L. Taravati, R.N. Zuckermann, Molecular Engineering of the Peptoid Nanosheet Hydrophobic Core, Langmuir 32(45) (2016) 11946-11957.

[34] H. Jin, F. Jiao, M.D. Daily, Y. Chen, F. Yan, Y.-H. Ding, X. Zhang, E.J. Robertson, M.D. Baer, C.-L. Chen, Highly stable and self-repairing membrane-mimetic 2D nanomaterials assembled from lipid-like peptoids, Nat. Commun. 7 (2016) 12252.

[35] T.S. Burkoth, A.T. Fafarman, D.H. Charych, M.D. Connolly, R.N. Zuckermann, Incorporation of Unprotected Heterocyclic Side Chains into Peptoid Oligomers via Solid-Phase Submonomer Synthesis, J. Am. Chem. Soc. 125(29) (2003) 8841-8845.

[36] C.W. Wu, T.J. Sanborn, K. Huang, R.N. Zuckermann, A.E. Barron, Peptoid Oligomers with α-Chiral, Aromatic Side Chains: Sequence Requirements for the Formation of Stable Peptoid Helices, J. Am. Chem. Soc. 123(28) (2001) 6778-6784.

[37] K. Kirshenbaum, A.E. Barron, R.A. Goldsmith, P. Armand, E.K. Bradley, K.T.V. Truong, K.A. Dill, F.E. Cohen, R.N. Zuckermann, Sequence-specific polypeptoids: A diverse family of heteropolymers with stable secondary structure, Proc. Natl. Acad. Sci. 95(8) (1998) 4303-4308.

[38] R.N. Zuckermann, E.J. Martin, D.C. Spellmeyer, G.B. Stauber, K.R. Shoemaker, J.M. Kerr, G.M. Figliozzi, D.A. Goff, M.A. Siani, Discovery of Nanomolar Ligands for 7-Transmembrane G-Protein-Coupled Receptors from a Diverse N-(Substituted)glycine Peptoid Library, J. Med. Chem. 37(17) (1994) 2678-2685.

[39] T.S. Burkoth, E. Beausoleil, S. Kaur, D. Tang, F.E. Cohen, R.N. Zuckermann, Toward the Synthesis of Artificial Proteins: The Discovery of an Amphiphilic Helical Peptoid Assembly, Chem. Biol. 9(5) (2002) 647-654.

[40] T.M. Doran, P. Dickson, J.M. Ndungu, P. Ge, I. Suponitsky-Kroyter, H. An, T. Kodadek, Chapter Five - Synthesis and screening of bead-displayed combinatorial libraries, in: A.K. Shukla (Ed.), Methods Enzymol., Academic Press2019, pp. 91-127.

[41] M.G. Paulick, K.M. Hart, K.M. Brinner, M. Tjandra, D.H. Charych, R.N. Zuckermann, Cleavable Hydrophilic Linker for One-Bead-One-Compound Sequencing of Oligomer Libraries by Tandem Mass Spectrometry, J. Comb. Chem. 8(3) (2006) 417-426.

[42] T.M. Ross, R.N. Zuckermann, C. Reinhard, W.H. Frey, Intranasal administration delivers peptoids to the rat central nervous system, Neurosci. Lett. 439(1) (2008) 30-33.

[43] A.C. Raymond, B. Gao, L. Girard, J.D. Minna, D. Gomika Udugamasooriya, Unbiased peptoid combinatorial cell screen identifies plectin protein as a potential biomarker for lung cancer stem cells, Sci. Rep. 9(1) (2019) 14954.

[44] C.W. Wu, T.J. Sanborn, R.N. Zuckermann, A.E. Barron, Peptoid Oligomers with α-Chiral, Aromatic Side Chains: Effects of Chain Length on Secondary Structure, J. Am. Chem. Soc. 123(13) (2001) 2958-2963.

[45] J.A. Crapster, I.A. Guzei, H.E. Blackwell, A Peptoid Ribbon Secondary Structure, Angew. Chem. Int. Ed. 52(19) (2013) 5079-5084.

[46] B.C. Gorske, E.M. Mumford, C.G. Gerrity, I. Ko, A Peptoid Square Helix via Synergistic Control of Backbone Dihedral Angles, J. Am. Chem. Soc. 139(24) (2017) 8070-8073.

[47] J. Sun, A.A. Teran, X. Liao, N.P. Balsara, R.N. Zuckermann, Nanoscale Phase Separation in Sequence-Defined Peptoid Diblock Copolymers, J. Am. Chem. Soc. 135(38) (2013) 14119-14124.

[48] J. Sun, A.A. Teran, X. Liao, N.P. Balsara, R.N. Zuckermann, Crystallization in Sequence-Defined Peptoid Diblock Copolymers Induced by Microphase Separation, J. Am. Chem. Soc. 136(5) (2014) 2070-2077.

[49] J. Sun, X. Liao, A.M. Minor, N.P. Balsara, R.N. Zuckermann, Morphology-Conductivity Relationship in Crystalline and Amorphous Sequence-Defined Peptoid Block Copolymer Electrolytes, J. Am. Chem. Soc. 136(42) (2014) 14990-14997.

[50] C.-U. Lee, A. Li, K. Ghale, D. Zhang, Crystallization and Melting Behaviors of Cyclic and Linear Polypeptoids with Alkyl Side Chains, Macromolecules 46(20) (2013) 8213-8223.

[51] X. Jiang, D.R. Greer, J. Kundu, C. Ophus, A.M. Minor, D. Prendergast, R.N. Zuckermann, N.P. Balsara, K.H. Downing, Imaging Unstained Synthetic Polymer Crystals and Defects on Atomic Length Scales Using Cryogenic Electron Microscopy, Macromolecules 51(19) (2018) 7794-7799.

[52] X. Jiang, S. Xuan, J. Kundu, D. Prendergast, R.N. Zuckermann, N.P. Balsara, Effect of processing and end groups on the crystal structure of polypeptoids studied by cryogenic electron microscopy at atomic length scales, Soft Matter 15(23) (2019) 4723-4736.

[53] V. Castelletto, J. Seitsonen, K.M. Tewari, A. Hasan, R.M. Edkins, J. Ruokolainen, L.M. Pandey, I.W. Hamley, K.H.A. Lau, Self-Assembly of Minimal Peptoid Sequences, ACS Macro Lett. 9(4) (2020) 494-499.

[54] V. Castelletto, A.M. Chippindale, I.W. Hamley, S. Barnett, A. Hasan, K.H.A. Lau, Crystallization and lamellar nanosheet formation of an aromatic dipeptoid, Chem. Commun. 55(42) (2019) 5867-5869.

[55] J. Sun, X. Jiang, R. Lund, K.H. Downing, N.P. Balsara, R.N. Zuckermann, Self-assembly of crystalline nanotubes from monodisperse amphiphilic diblock copolypeptoid tiles, Proc. Natl. Acad. Sci. 113(15) (2016) 3954-3959.

[56] H. Jin, Y.-H. Ding, M. Wang, Y. Song, Z. Liao, C.J. Newcomb, X. Wu, X.-Q. Tang, Z. Li, Y. Lin, F. Yan, T. Jian, P. Mu, C.-L. Chen, Designable and dynamic single-walled stiff nanotubes assembled from sequence-defined peptoids, Nat. Commun. 9(1) (2018) 270.

[57] Y. Deng, H. Chen, X. Tao, F. Cao, S. Trépout, J. Ling, M.-H. Li, Oxidation-Sensitive Polymersomes Based on Amphiphilic Diblock Copolypeptoids, Biomacromolecules 20(9) (2019) 3435-3444.

[58] X. Jiang, R.K. Spencer, J. Sun, C. Ophus, R.N. Zuckermann, K.H. Downing, N.P. Balsara, Resolving the Morphology of Peptoid Vesicles at the 1 nm Length Scale Using Cryogenic Electron Microscopy, J. Phys. Chem. B 123(5) (2019) 1195-1205.

[59] H.K. Murnen, A.M. Rosales, J.N. Jaworski, R.A. Segalman, R.N. Zuckermann, Hierarchical Self-Assembly of a Biomimetic Diblock Copolypeptoid into Homochiral Superhelices, J. Am. Chem. Soc. 132(45) (2010) 16112-16119.

[60] G.L. Sternhagen, S. Gupta, Y. Zhang, V. John, G.J. Schneider, D. Zhang, Solution Self-Assemblies of Sequence-Defined Ionic Peptoid Block Copolymers, J. Am. Chem. Soc. 140(11) (2018) 4100-4109.

[61] R.K. Spencer, G.L. Butterfoss, J.R. Edison, J.R. Eastwood, S. Whitelam, K. Kirshenbaum, R.N. Zuckermann, Stereochemistry of polypeptoid chain configurations, Biopolymers 110(6) (2019) e23266.

[62] D.R. Greer, M.A. Stolberg, J. Kundu, R.K. Spencer, T. Pascal, D. Prendergast, N.P. Balsara, R.N. Zuckermann, Universal Relationship between Molecular Structure and Crystal Structure in Peptoid Polymers and Prevalence of the cis Backbone Conformation, J. Am. Chem. Soc. 140(2) (2018) 827-833.

[63] J.R. Edison, R.K. Spencer, G.L. Butterfoss, B.C. Hudson, A.I. Hochbaum, A.K. Paravastu, R.N. Zuckermann, S. Whitelam, Conformations of peptoids in nanosheets result from the interplay of backbone energetics and intermolecular interactions, Proc. Natl. Acad. Sci. 115(22) (2018) 5647-5651.

[64] B.C. Hudson, A. Battigelli, M.D. Connolly, J. Edison, R.K. Spencer, S. Whitelam, R.N. Zuckermann, A.K. Paravastu, Evidence for cis Amide Bonds in Peptoid Nanosheets, J. Phys. Chem. Lett. 9(10) (2018) 2574-2578.

[65] A.M. Rosales, B.L. McCulloch, R.N. Zuckermann, R.A. Segalman, Tunable Phase Behavior of Polystyrene–Polypeptoid Block Copolymers, Macromolecules 45(15) (2012) 6027-6035.

[66] K.T. Nam, S.A. Shelby, P.H. Choi, A.B. Marciel, R. Chen, L. Tan, T.K. Chu, R.A. Mesch, B.-C. Lee, M.D. Connolly, C. Kisielowski, R.N. Zuckermann, Free-floating ultrathin two-dimensional crystals from sequence-specific peptoid polymers, Nat. Mater. 9(5) (2010) 454-460.

[67] E.J. Robertson, G.K. Olivier, M. Qian, C. Proulx, R.N. Zuckermann, G.L. Richmond, Assembly and molecular order of two-dimensional peptoid nanosheets through the oil–water interface, Proc. Natl. Acad. Sci. 111(37) (2014) 13284-13289.

[68] B. Sanii, T.K. Haxton, G.K. Olivier, A. Cho, B. Barton, C. Proulx, S. Whitelam, R.N. Zuckermann, Structure-Determining Step in the Hierarchical Assembly of Peptoid Nanosheets, ACS Nano 8(11) (2014) 11674-11684.

[69] R.V. Mannige, T.K. Haxton, C. Proulx, E.J. Robertson, A. Battigelli, G.L. Butterfoss, R.N. Zuckermann, S. Whitelam, Peptoid nanosheets exhibit a new secondary-structure motif, Nature 526(7573) (2015) 415-420.

[70] B. Sanii, R. Kudirka, A. Cho, N. Venkateswaran, G.K. Olivier, A.M. Olson, H. Tran, R.M. Harada, L. Tan, R.N. Zuckermann, Shaken, Not Stirred: Collapsing a Peptoid Monolayer To Produce Free-Floating, Stable Nanosheets, J. Am. Chem. Soc. 133(51) (2011) 20808-20815.

[71] E.J. Robertson, E.M. Nehls, R.N. Zuckermann, Structure–Rheology Relationship in Nanosheet-Forming Peptoid Monolayers, Langmuir 32(46) (2016) 12146-12158.

[72] D. Flood, C. Proulx, E.J. Robertson, A. Battigelli, S. Wang, A.M. Schwartzberg, R.N. Zuckermann, Improved chemical and mechanical stability of peptoid nanosheets by photo-crosslinking the hydrophobic core, Chem. Commun. 52(26) (2016) 4753-4756.

[73] Y. Cong, S.J. Ludtke, Chapter Eight - Single Particle Analysis at High Resolution, in: G.J. Jensen (Ed.), Methods Enzymol., Academic Press2010, pp. 211-235.

[74] S. Hoyas, V. Lemaur, Q. Duez, F. Saintmont, E. Halin, J. De Winter, P. Gerbaux, J. Cornil, PEPDROID: Development of a Generic DREIDING-Based Force Field for the Assessment of Peptoid Secondary Structures, Adv. Theory Simul. 1(12) (2018) 1800089.

[75] L.J. Weiser, E.E. Santiso, A CGenFF-based force field for simulations of peptoids with both cis and trans peptide bonds, J. Comput. Chem. 40(22) (2019) 1946-1956.

[76] S. Xuan, X. Jiang, R.K. Spencer, N.K. Li, D. Prendergast, N.P. Balsara, R.N. Zuckermann, Atomic-level engineering and imaging of polypeptoid crystal lattices, Proc. Natl. Acad. Sci. 116(45) (2019) 22491-22499.

[77] A. Battigelli, J.H. Kim, D.C. Dehigaspitiya, C. Proulx, E.J. Robertson, D.J. Murray, B. Rad, K. Kirshenbaum, R.N. Zuckermann, Glycosylated Peptoid Nanosheets as a Multivalent Scaffold for Protein Recognition, ACS Nano 12(3) (2018) 2455-2465.

[78] J.H. Kim, E.M. Grzincic, L. Yun, R.K. Spencer, M.A. Kline, R.N. Zuckermann, Lipid-anchor display on peptoid nanosheets via co-assembly for multivalent pathogen recognition, Soft Matter 16(4) (2020) 907-913.

[79] J.H. Kim, S.C. Kim, M.A. Kline, E.M. Grzincic, B.W. Tresca, J. Cardiel, M. Karbaschi, D.C. Dehigaspitiya, Y. Chen, V. Udumula, T. Jian, D.J. Murray, L. Yun, M.D. Connolly, J. Liu, G. Ren, C.-L. Chen, K. Kirshenbaum, A.R. Abate, R.N. Zuckermann, Discovery of Stable and Selective Antibody Mimetics from Combinatorial Libraries of Polyvalent, Loop-Functionalized Peptoid Nanosheets, ACS Nano 14(1) (2020) 185-195.

[80] F. Jiao, Y. Chen, H. Jin, P. He, C.-L. Chen, J.J. De Yoreo, Self-Repair and Patterning of 2D Membrane-Like Peptoid Materials, Adv. Funct. Mater. 26(48) (2016) 8960-8967.

[81] L. Chio, J.T. Del Bonis-O'Donnell, M.A. Kline, J.H. Kim, I.R. McFarlane, R.N. Zuckermann, M.P. Landry, Electrostatic Assemblies of Single-Walled Carbon Nanotubes and Sequence-Tunable Peptoid Polymers Detect a Lectin Protein and Its Target Sugars, Nano Lett. 19(11) (2019) 7563-7572.

[82] S.-T. Wang, M.A. Gray, S. Xuan, Y. Lin, J. Byrnes, A.I. Nguyen, N. Todorova, M.M. Stevens, C.R. Bertozzi, R.N. Zuckermann, O. Gang, DNA origami protection and molecular interfacing through engineered sequence-defined peptoids, Proc. Natl. Acad. Sci. 117(12) (2020) 6339-6348.

[83] C.J. Jimenez, J. Tan, K.M. Dowell, G.E. Gadbois, C.A. Read, N. Burgess, J.E. Cervantes, S. Chan, A. Jandaur, T. Karanik, J.J. Lee, M.C. Ley, M. McGeehan, A. McMonigal, K.L. Palazzo, S.A. Parker, A. Payman, M. Soria, L. Verheyden, V.T. Vo, J. Yin, A.L. Calkins, A.A. Fuller, G.Y. Stokes, Peptoids advance multidisciplinary research and undergraduate education in parallel: Sequence effects on conformation and lipid interactions, Biopolymers 110(4) (2019) e23256.

[84] D.J. Murray, J.H. Kim, E.M. Grzincic, S.C. Kim, A.R. Abate, R.N. Zuckermann, Uniform, Large-Area, Highly Ordered Peptoid Monolayer and Bilayer Films for Sensing Applications, Langmuir 35(42) (2019) 13671-13680.

[85] K.J. Prathap, G. Maayan, Metallopeptoids as efficient biomimetic catalysts, Chem. Commun. 51(55) (2015) 11096-11099.

[86] S.C. Young, A Systematic Review of Antiamyloidogenic and Metal-Chelating Peptoids: Two Structural Motifs for the Treatment of Alzheimer's Disease, Molecules 23(2) (2018) 296.

[87] G. Maayan, M.D. Ward, K. Kirshenbaum, Metallopeptoids, Chem. Commun. (1) (2009) 56-58.

[88] A.S. Knight, E.Y. Zhou, J.G. Pelton, M.B. Francis, Selective Chromium(VI) Ligands Identified Using Combinatorial Peptoid Libraries, J. Am. Chem. Soc. 135(46) (2013) 17488-17493.

[89] M. Baskin, H. Zhu, Z.-W. Qu, J.H. Chill, S. Grimme, G. Maayan, Folding of unstructured peptoids and formation of hetero-bimetallic peptoid complexes upon side-chain-to-metal coordination, Chem. Sci. 10(2) (2019) 620-632.

[90] T. Ghosh, N. Fridman, M. Kosa, G. Maayan, Self-Assembled Cyclic Structures from Copper(II) Peptoids, Angew. Chem. 130(26) (2018) 7829-7834.

[91] A.I. Nguyen, R.K. Spencer, Christopher L. Anderson, R.N. Zuckermann, A bio-inspired approach to ligand design: folding single-chain peptoids to chelate a multimetallic cluster, Chem. Sci. 9(47) (2018) 8806-8813.

[92] B.C. Gorske, J.R. Stringer, B.L. Bastian, S.A. Fowler, H.E. Blackwell, New Strategies for the Design of Folded Peptoids Revealed by a Survey of Noncovalent Interactions in Model Systems, J. Am. Chem. Soc. 131(45) (2009) 16555-16567.

[93] O. Roy, C. Caumes, Y. Esvan, C. Didierjean, S. Faure, C. Taillefumier, The tert-Butyl Side Chain: A Powerful Means to Lock Peptoid Amide Bonds in the Cis Conformation, Org. Lett. 15(9) (2013) 2246-2249.

[94] C. Caumes, O. Roy, S. Faure, C. Taillefumier, The Click Triazolium Peptoid Side Chain: A Strong cis-Amide Inducer Enabling Chemical Diversity, J. Am. Chem. Soc. 134(23) (2012) 9553-9556.

[95] J.R. Stringer, J.A. Crapster, I.A. Guzei, H.E. Blackwell, Construction of Peptoids with All Trans-Amide Backbones and Peptoid Reverse Turns via the Tactical Incorporation of N-Aryl Side Chains Capable of Hydrogen Bonding, J. Org. Chem. 75(18) (2010) 6068-6078.

[96] B. Paul, G.L. Butterfoss, M.G. Boswell, M.L. Huang, R. Bonneau, C. Wolf, K. Kirshenbaum, N-Naphthyl Peptoid Foldamers Exhibiting Atropisomerism, Org. Lett. 14(3) (2012) 926-929.

[97] A.W. Wijaya, A.I. Nguyen, L.T. Roe, G.L. Butterfoss, R.K. Spencer, N.K. Li, R.N. Zuckermann, Cooperative Intramolecular Hydrogen Bonding Strongly Enforces cis-Peptoid Folding, J. Am. Chem. Soc. 141(49) (2019) 19436-19447.

[98] S.C. Leguizamon, T.F. Scott, Sequence-selective dynamic covalent assembly of information-bearing oligomers, Nat. Commun. 11(1) (2020) 784.